Astron. Astrophys. 357, 1137–1142 (2000)

ASTRONOMY AND ASTROPHYSICS

Experimental transition probabilities of several NeI lines

J.A. del Val⋆**, J.A. Aparicio, V. González, and S. Mar**

Departamento de Optica, Facultad de Ciencias, Universidad de Valladolid, 47071 Valladolid, Spain

Received 8 November 1999 / Accepted 28 February 2000

Abstract. This work reports a collection of 28 transition probabilities of lines in the spectral region 590–815 nm, corresponding to the most intense Ne I transitions (3p-3s, 3d-3p), all measured in an emission experiment. Relative intensity measurements have been made on a pulsed discharge lamp and the absolute A_{ki} values have been obtained by using an extensive set of data taken from the literature. The electron density has been determined by one-wavelength interferometry and ranges from 0.1 to $1.8 \times 10^{23}\mathrm{m}^{-3}$ in the plasma. The NeI excitation temperature $(11000$–$21000\,K)$ has been determined from the Boltzmann-plot of the lines and also estimated by the Saha law.

Key words: atomic data – line: profiles – methods: laboratory

1. Introduction

Neon is one of the more abundant elements in the universe; it is a member of the α-chain and accurate knowledge of its abundance is of primary interest in studies of stellar nucleosynthesis. Moreover, it is frequently used in laboratory studies and in industrial applications. There has been considerable interest in transition probabilities for Ne states since the first laser oscillation on Ne transitions was obtained in 1961. Although there are numerous determinations of lifetimes of individual Ne states and a considerable bibliography on atomic transition probabilities, many of the available experimental studies present some discrepancies with theoretical works. Undoubtedly, reliable transition probabilities are needed for spectroscopic diagnostics of plasmas.

In the present work we have used the intensities of a NeI plasma emission to determine relative transition probabilities which are then compared with an extensive collection of both experimental and theoretical values reported in the literature. The plasma seems to be well described by a partial local thermodynamic equilibrium model. The absence of self-absorption and the spectral calibration have been very carefully taken in account (del Val et al. 1999; Aparicio et al. 1997). The high number of measurements (25) performed for each line along the plasma life, and its very controlled features, allows us to obtain a very good A_{ki} value by the mean value, and its uncertainty by the standard deviation (usually $< 10\%$).

2. Experimental arrangement

All measurements have been made in a pulsed discharge lamp. The experimental set-up (shown in Fig. 1) and the methods have already been described in Gigosos et al. (1994) and Aparicio et al. (1997). Also, the specific details corresponding to the present experiment have been reported in del Val et al. (1999). Thus, here we only summarize some of these details.

The source of plasma consists of a cylindrical tube of Pyrex glass, 175 mm in length and 19 mm in interior diameter. The lamp has been designed to avoid sputtering as much as possible. The plasmas were created by discharging a capacitor bank of 20 μF charged up to 6.5 kV. During the whole experiment the lamp was working with a continuous flow of a mixture of neon and helium, at a rate of 10 cm^3/min, and a pressure of 40 mbar. Partial pressures Ne:He (1:9) were selected to avoid self-absorption. Under these conditions, the plasma emission lasted for 450 μs. The gas was pre-ionised in order to obtain the best discharge reliability. Spectroscopic and interferometric end-on measurements have been made simultaneously through the plasma life, and have been taken 2 mm off the lamp axis, and from symmetrical positions referred to it. The high axial homogeneity and the very good cylindrical symmetry of electron density and temperature in this lamp allows this (del Val et al. 1998).

According to Fig. 1, the lamp is placed in one of the arms of a Twyman-Green interferometer illuminated with an argon ion laser (488.0 nm). The spectroscopic beam is directed (3 mm pinholes D2, D3, separated 1.5 m) and focused (cylindrical lens L2 with 150 mm focal length) onto the entrance slit of a Jobin-Yvon spectrometer (1.5 m focal length, 1200 lines/mm holographic grating), equipped with an optical multichannel analyser (OMA). This OMA has a detector array which is divided into 512 channels (EG&G 1455R-512-HQ). The dispersion was 12.59 pm/channel at 589.0 nm in first order of diffraction. The spectrometer was very carefully calibrated in wavelength as well as in intensity (Aparicio et al. 1997; del Val 1997). Time exposures for the spectra were 5 μs. Mirror M4, placed behind the

Send offprint requests to: J.A. Aparicio

⋆ *Present address:* Departamento de Física Aplicada, Universidad de Salamanca, E. Politécnica Superior 05071 Avila, Spain

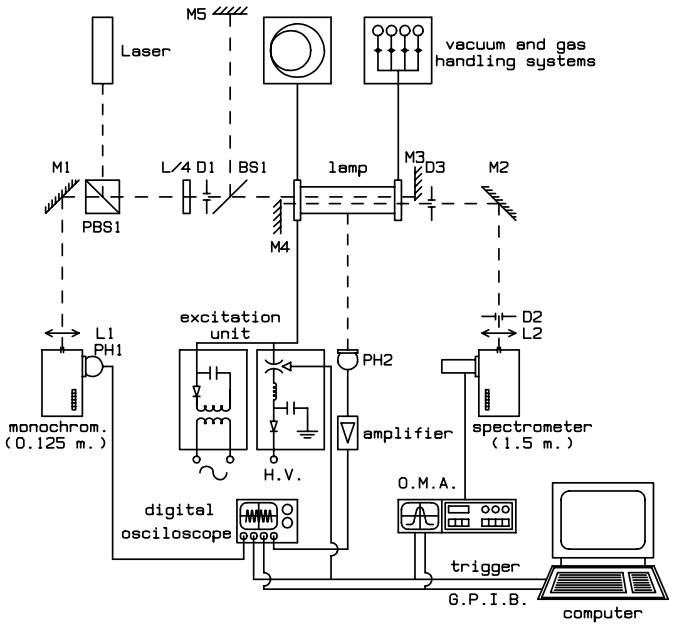

Fig. 1. Experimental set-up

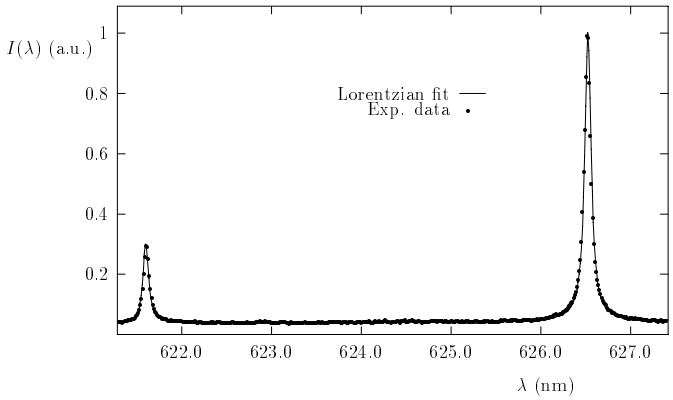

Fig. 2. Experimental spectrum and its Lorentzian fit. This spectral record shows the NeI 621.73 and 626.65 nm lines emitted at the instant 90 μs of the plasma life

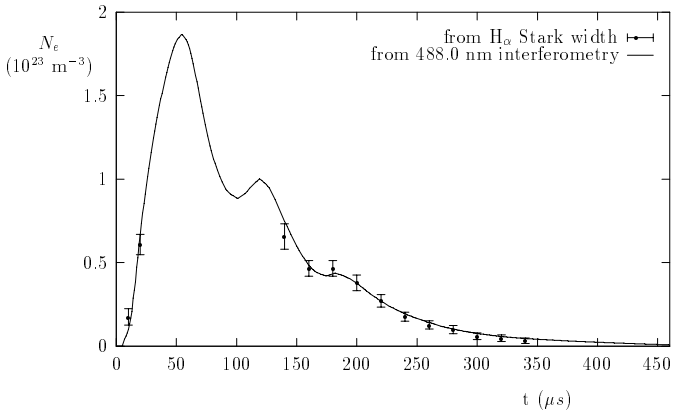

Fig. 3. Electron density evolution measured from interferometry and from H_α-Stark broadening

plasma column, was used to measure the optical depth and to detect possible self-absorption effects on each line profile. This can be done by comparing the spectra taken with and without the light reflected by this mirror (González et al. 1989).

3. Measurements and plasma diagnostics

The experiment consists of end-on measurements of the NeI lines emitted by the plasma in the region 590–815 nm. Each spectral interval has been recorded at 25 different instants of the plasma lifetime. For each instant, we have made six runs, three of them with the mirror M4 and the other three without it, in order to test for self-absorption in all measurements. An example of a spectrum recorded for the NeI 621.73 nm and 626.65 nm lines at 90 μs of the plasma life is shown in Fig. 2. Due to the presence of hydrogen impurities in the neon plasma, it has also been possible to make measurements of the H_α profiles, whose Stark broadening has allowed us to determine the electron density spectroscopically. All the lines were registered in first order of diffraction of the spectrometer, the most efficient.

The complete experiment lasted around 20 hours. To control the plasma pulse reproducibility, spectra corresponding to 5 different NeI lines (621.73, 626.65, 638.30, 640.22 and 748.89 nm) were registered at the 25 different instants of the plasma lifetime, in regular intervals of 3 hours. Also, 75 interferometric registers (1 ms long) of the plasma refractivity were recorded. These have been used to determine the electron density. By comparing the seven electron density curves, dispersions lower than 6% were found; meanwhile the comparison of the intensities (areas below the profiles) for each of the 5 NeI lines resulted in dispersions below 9%. Furthermore, no trends were observed in these control parameters, which gives an idea of the good performance of this plasma source.

As a first step, self-absorption has been checked in all recorded spectra. The technique described in González et al. (1989) has been used, showing this effect to be almost negligible. In fact, corrections performed in peak intensities are lower than 10%, and it affects only up to around 5% of the spectra considered in further calculations. Afterwards, the spectra were divided by the spectrometer transmittance and fitted to sums of Lorentzian functions plus a luminous background with a linear dependence, as explained in reference (Gigosos et al. 1994). Differences between the experimental spectra and the fits were usually lower than 1% (see Fig. 2). These fitting algorithms allow us to determine simultaneously the center, asymmetry, linewidth and area of each profile.

Fig. 3 shows the electron density N_e, determined interferometrically at a single-wavelength (488.0 nm) and spectroscopically from H_α Stark broadening (Gigosos & Cardenoso 1996). The spectroscopic electron density is shown for those instants where N_e is lower than $0.7 \times 10^{23}\,\mathrm{m}^{-3}$. Only in these cases the Balmer-alpha wings and background are entirely registered in the spectra, and so, its linewidth can be properly determined. As is shown in this figure, very good agreement between both

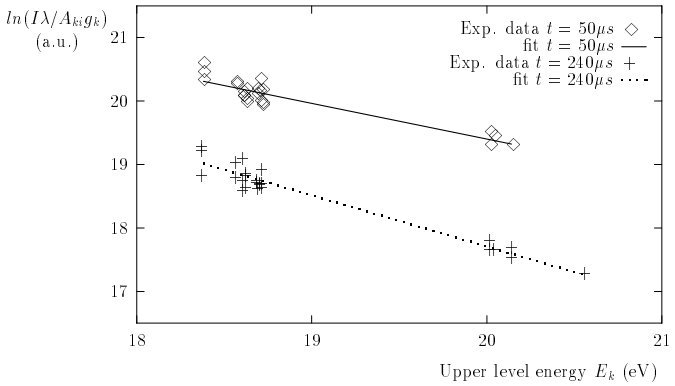

Fig. 4. Two examples of NeI Boltzmann-plots corresponding to the plasmalife instants 50 and 240 μs. The good point distribution along the straigh lines for each case, show that excitation temperature follows the Boltzmann law for these levels

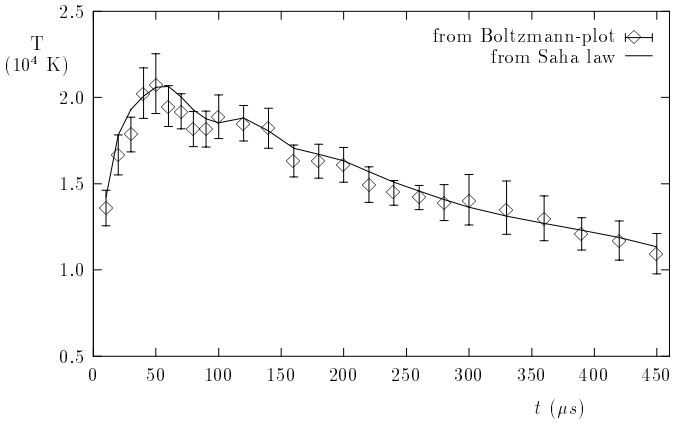

Fig. 5. Temperature evolution measured from the Boltzmann-plots of NeI lines and also estimated from the Saha law

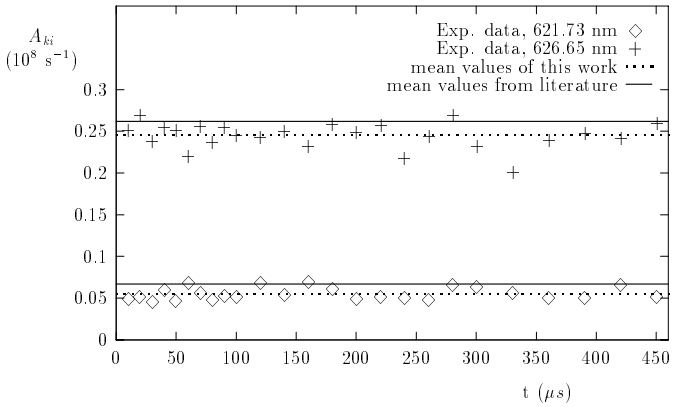

Fig. 6. A_{ki} data of this study, corresponding to the NeI 621.73 and 626.65 nm lines, already shown in Fig. 2, versus time of the plasma life. No trends are observed and there is a good agreement with literature mean values

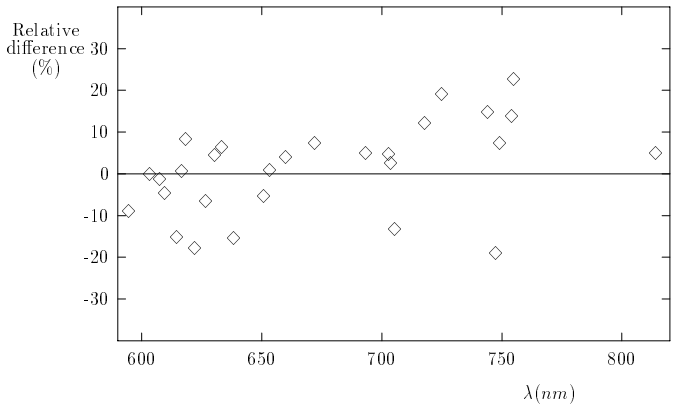

Fig. 7. Relative differences between A_{ki} mean values of this study and literature mean values versus λ. No trends are detected

methods is observed. 10% is a good estimation for the electron density uncertainty.

In collision-dominated plasmas like the one generated in this experiment, it is a common hypothesis to assume that excitation temperature, Saha temperature and kinetic electron temperature take similar values (Van der Mullen 1990). In this study we have determined the NeI excitation temperature from the slope of a Boltzmann-plot calculated with the intensities of a selected set of 25 NeI lines, for each instant of the plasma lifetime (see Fig. 4). The Boltzmann-plot requires a previous knowledge of the transition probabilities for the lines represented. Hence, we have choosen for each line the mean value between the different available A_{ki} in the literature (a mean value between 27 authors). In this way, the accuracy of our Boltzmann-plots mainly comes from the many data taken in the procedure. The Saha temperature has been estimated from the experimental electron density and the filling pressure. Both temperatures agree well and are shown in Fig. 5. This agreement suggests that the levels involved in the Boltzmann calculations are well described by a partial local thermodynamic equilibrium (pLTE) model. Finally, the error estimated for the temperature is around 10%. In Fig. 5 the temperature error bars have been obtained from dispersion values corresponding to the slope in the linear fit performed for each Boltzmann-plot (see Fig. 4).

4. Results and conclusions

Table 1 summarizes our results, including values collected from the literature, where the columns are headed by their author reference. These references, listed in the table footer, have been arranged following two criteria:

First, references are listed beginning with the experimental works, that appear in the first two horizontal lines for each transition, references 1 to 16. After this, the theoretical studies appear in the second and third horizontal lines for each transition, references 17 to 27.

Second, in both cases citations are ordered chronologically.

Also, the mean value of all the listed references is shown with its standard deviation. These are the values taken in Boltzmann-plot calculations in order to obtain the temperature.

The uncertainty for each A_{ki} value of this experiment can be evaluated by the standard deviations that show the 25 different experimental values for each line. Although with a clear dependence on the line, usually these uncertainties are below 10%.

Table 1. A_{ki}-values from literature and from this work. All values must be multiplied by $10^8\ s^{-1}$.

λ (nm)	upper level	lower level	(1) (10) (19)	(2) (11) (20)	(3) (12) (21)	(4) (13) (22)	(5) (14) (23)	(6) (15) (24)	(7) (16) (25)	(8) (17) (26)	(9) (18) (27)	$\langle A_{ki}\rangle$ lit.	σ (%)	$\langle A_{ki}\rangle$ this work	σ (%)
594.48	$3p'(3/2)$	$3s(3/2)^\circ$	0.105	0.090	0.105	0.099	0.112	0.107	0.107	0.099	0.113	0.112	11	0.102	7
			0.108	0.103	0.103		0.121	0.124	0.100						
			0.126	0.134	0.117	0.136				0.130	0.109				
603.00	$3p'(1/2)$	$3s(3/2)^\circ$	0.063	0.048	0.050		0.051	0.045	0.062	0.046	0.056	0.054	12	0.054	9
			0.058	0.051	0.050		0.047	0.055	0.052						
			0.051	0.066	0.057	0.065				0.048	0.052				
607.43	$3p(1/2)$	$3s(3/2)^\circ$	0.617	0.560	0.480	0.580	0.583	0.558	0.590	0.552	0.603	0.583	8	0.576	8
			0.465		0.603		0.572	0.567	0.570						
			0.590	0.666	0.597	0.676			0.615	0.625	0.568				
609.62	$3p'(3/2)$	$3s(3/2)^\circ$	0.169	0.156	0.160	0.168	0.179	0.166	0.172	0.153	0.181	0.175	9	0.167	8
			0.163	0.171	0.158		0.178	0.180	0.178						
			0.166	0.209	0.186	0.211				0.197	0.175				
614.31	$3p(3/2)$	$3s(3/2)^\circ$	0.216	0.231	0.275	0.220	0.285	0.289	0.276	0.266	0.283	0.290	21	0.246	17
			0.268	0.291	0.291		0.293	0.300	0.270						
			0.268	0.325	0.294	0.329			0.525	0.305	0.280				
616.36	$3p'(1/2)$	$3s'(1/2)^\circ$	0.160	0.153	0.150	0.135	0.141	0.149	0.173	0.142	0.146	0.149	12	0.150	8
			0.131	0.135	0.120		0.151	0.147	0.149						
			0.151	0.172	0.155	0.172			0.195	0.113	0.142				
618.21	$5s(3/2)^\circ$	$3p(5/2)$										0.036	0	0.039	10
					0.036										
								0.036	0.036		0.036				
621.73	$3p(3/2)$	$3s(3/2)^\circ$	0.078	0.052			0.060				0.064	0.067	16	0.055	13
				0.065	0.072		0.062	0.061	0.063						
									0.094	0.068	0.061				
626.65	$3p'(3/2)$	$3s'(1/2)^\circ$	0.223	0.227			0.254				0.250	0.262	16	0.245	6
				0.243	0.262		0.259	0.252	0.250						
									0.373	0.306	0.242				
630.48	$3p(3/2)$	$3s(3/2)^\circ$	0.051	0.045	0.038	0.048	0.042	0.040	0.049	0.037	0.042	0.044	11	0.046	9
			0.043	0.042	0.041		0.045	0.041	0.045						
			0.053	0.045	0.042	0.047			0.055	0.040	0.042				
633.44	$3p(3/2)$	$3s(3/2)^\circ$	0.136	0.164	0.140	0.147	0.180	0.164	0.146	0.149	0.161	0.160	17	0.170	9
			0.165	0.172	0.169		0.179	0.183	0.165						
			0.159	0.185	0.172	0.188			0.053	0.174	0.161				
638.30	$3p(3/2)$	$3s(3/2)^\circ$	0.279	0.303			0.316				0.322	0.336	12	0.284	7
				0.360	0.360		0.326	0.330	0.320						
									0.447	0.351	0.317				
650.65	$3p(5/2)$	$3s(3/2)^\circ$	0.232	0.289	0.222	0.246	0.298	0.308	0.254	0.279	0.301	0.300	16	0.284	9
			0.270	0.320	0.320		0.301	0.298	0.290						
			0.298	0.334	0.320	0.339			0.454	0.325	0.292				
653.29	$3p'(3/2)$	$3s'(1/2)^\circ$	0.128	0.119			0.106				0.108	0.111	9	0.112	6
				0.116	0.125		0.106	0.103	0.099						
										0.112	0.100				
659.90	$3p'(1/2)$	$3s'(1/2)^\circ$	0.251	0.249	0.235	0.224	0.225	0.234	0.244	0.219	0.233	0.239	12	0.248	6
			0.201	0.217	0.217		0.240	0.231	0.240						
			0.214	0.240	0.234	0.248			0.332	0.305	0.226				
671.70	$3p'(3/2)$	$3s'(1/2)^\circ$	0.234	0.238			0.217				0.217	0.216	11	0.232	6
				0.227	0.227		0.222	0.228	0.220						
									0.158	0.182	0.218				
692.95	$3p(3/2)$	$3s'(1/2)^\circ$	0.190	0.231	0.180	0.165	0.174	0.179	0.211	0.166	0.174	0.185	8	0.194	7
			0.177	0.193	0.178		0.178	0.175	0.186						
			0.173	0.192	0.197	0.195				0.199	0.176				
702.40	$3p(3/2)$	$3s'(1/2)^\circ$		0.030			0.020				0.019	0.021	18	0.022	8
				0.023	0.023		0.019	0.019	0.018						
										0.017	0.020				

Table 1. (continued)

λ (nm)	upper level	lower level	(1) (10) (19)	(2) (11) (20)	(3) (12) (21)	(4) (13) (22)	(5) (14) (23)	(6) (15) (24)	(7) (16) (25)	(8) (17) (26)	(9) (18) (27)	$\langle A_{ki} \rangle$ lit.	σ (%)	$\langle A_{ki} \rangle$ this work	σ (%)
703.24	$3p(1/2)$	$3s(3/2)^\circ$	0.192		0.200	0.198	0.253	0.275	0.206	0.235	0.253	0.253	14	0.259	10
			0.265	0.258	0.258				0.260						
			0.253	0.284	0.285	0.288			0.328	0.277	0.248				
705.13	$3d'(3/2)^\circ$	$3p(1/2)$									0.030	0.038	87	0.033	13
			0.020		0.021	0.036				0.036	0.130				
							0.030	0.030		0.022	0.024				
717.39	$3p(5/2)$	$3s'(1/2)^\circ$	0.036	0.051	0.031		0.032	0.033	0.045	0.030	0.029	0.033	19	0.037	8
			0.031	0.034	0.032		0.031	0.030	0.033						
			0.018	0.031	0.033	0.032				0.034	0.031				
724.52	$3p(1/2)$	$3s(3/2)^\circ$	0.098		0.072	0.096	0.100	0.091	0.095	0.078	0.093	0.094	13	0.112	9
			0.107	0.097	0.093				0.098						
			0.093	0.106	0.109	0.108			0.061	0.104	0.094				
743.89	$3p(1/2)$	$3s'(1/2)^\circ$	0.029				0.024	0.033	0.038	0.029	0.023	0.027	16	0.031	9
			0.028	0.024	0.022				0.027						
			0.022	0.026	0.027	0.026				0.026	0.023				
747.24	$3d(3/2)^\circ$	$3p(1/2)$									0.040	0.047	48	0.038	16
									0.080	0.037	0.030				
748.89	$3d(3/2)^\circ$	$3p(1/2)$	0.349									0.245	21	0.263	8
			0.194		0.213										
								0.270	0.239	0.221	0.231				
753.58	$3d(1/2)^\circ$	$3p(1/2)$									0.430	0.334	20	0.380	5
									0.316	0.282	0.306				
754.40	$3d(1/2)^\circ$	$3p(1/2)$										0.410	14	0.503	10
									0.475	0.367	0.387				
813.64	$3d'(5/2)^\circ$	$3p(1/2)$										0.160	39	0.168	13
			0.114			0.144				0.238	0.260				
								0.124		0.120	0.118				

References:

(1) Wiese W.L., Smith M.W., Glenon B.M., 1966, In: Atomic Transition Probabilities, Vol.1, NBS, Washington DC
(2) Bennett W.R., Kindlmann Jr. P.M., 1966, Phys. Rev. 149, 38
(3) Irwin J.C., Nodwell R.A., 1966, Can. J. Phys. 44, 1781
(4) Nodwell R.A., van Andel H.W.H., Robinson A.M, 1968, J. Quant. Spectrosc. Radiat. Transfer. 8, 859
(5) Bridges J.M., Wiese W.L., 1970, Phys. Rev. A 2, 285
(6) Shoffstall D.R., Ellis D.G., 1970, J. Opt. Soc. Am. 60, 894
(7) Bengtson R.D., Miller M.H., 1970, J. Opt. Soc. Am. 60, 1093
(8) Schectman R.M., Shoffstall D.R., Ellis D.G., et al., 1973, J. Opt. Soc. Am. 63, 80
(9) Inatsugu S., Holmes J.R., 1975, Phys. Rev. A 11, 26
(10) Martin P., Campos J., 1977, An. Fis. 73, 276
(11) Chang R.S.F., Setser D.W., 1980, J. Chem. Phys. 72, 4099
(12) Haak H.K., Zetzsch C., Stuhl F., 1980, Z. Naturforsch. 35a, 1337
(13) Wosinski L., 1983, Acta Phys. Polon. A64, 471
(14) Hartmetz P., Schmoranzer H., 1983, Phys. Lett. 93A, 405
(15) Kandela S.A., 1984, Physica 123C, 370
(16) Fujimoto T., Goto C., Uetani Y., et al., 1985, Physica 128C, 96
(17) Murphy P.W., 1968, J. Opt. Soc. Am. 58, 1200
(18) Krivchenkova V.S., 1968, Opt. Spektrosk. 25, 966
(19) Mehlhorn R., 1969, J. Opt. Soc. Am. 59, 1453
(20) Feneuille S., Klapisch M., Koenig E., et al., 1970, Physica 48, 571
(21) Koenig E., 1971, Phys. Lett. 34A, 285
(22) Loginov A.V., Gruzdev P.F., 1974, Opt. Spectrosc. 37, 467
(23) Woodyard J.R., Altech P.L., 1975, J. Phys. B 8, 718
(24) Lilly R.A., 1976, J. Opt. Soc. Am. 66, 245
(25) Magazzu A., Pirronello V., Strazzulla G., 1983, J. Quant. Spectrosc. Transfer 29, 375
(26) Hibbert A., Le Dourneuf M., Mohan M., 1993, At. Data Nucl. Data Tables 53, 23
(27) Seaton M.J., 1998, J. Phys. B: Atom. Mol. Opt. Phys. 31, 5315

For instance, Fig. 6 shows the 25 different A_{ki}-values measured for the two NeI lines showed in Fig. 2. In this Figure the mean values of literature and this work also appear.

Fig. 7 shows the relative differences between the mean values taken from literature and this study for each line, as function of wavelength. As can be seen, usually these differences are below 10%, that is, within the statistical uncertainties assigned to

each line. Only for 6 lines, the differences are greater than 15% and only for 1 of these lines it is greater than 20%. Also, Fig. 7 shows that there are no systematic trends in this experiment with wavelength, which gives an idea of the good spectral intensity callibration performed. As can be seen in the table, often, when small differences with literature appear, the values of this study tend to be closer to the other experimental studies than to the theoretical ones. Also, within theoretical studies, the best agreement appears with the more recent calculations of Hibbert et al. (1993) and Seaton (1998). Both of these sets of theoretical results are obtained using methods which are more sophisticated than previous ones. For instance, for the line 747.24 nm, there is a difference with the literature mean value of 19%, although the agreement with the other available experimental studies is much more better and also with the last two theoretical studies, in contrast to the not so recent theoretical value of Magazzu et al. (1983). Another remark should be made for the line 705.13 nm. As Table 1 shows, one of the theoretical studies (reference 18) gives a value around five times above the other nine available literature values. In this way, the mean literature value is overestimated (and dispersion is 87%).

Taking into account the uncertainties around 30% that NIST has assigned to all these studied NeI A_{ki}-values in the last compilation (DASNIST data base, 1990), the main remark that should be made is the very good agreement between the values of this study and the literature mean values, although the three main advantages of this experiment are the following:

a) The lower uncertainties ($<$10% for the majority of the lines) when compared with other works and with the dispersion around the mean values of literature (see Table 1)

b) The coherence of a unique emission experiment, very carefully performed and with good plasma diagnostics, that furnishes an extensive set of data for each line, and this for many lines.

c) Finally, this experiment improves the knowledge of A_{ki}-values of those lines, like the last listed in Table 1, where there are very few references. Moreover, in some critical cases (for instance line 754.40 nm NeI) the present work supplies an experimental value opposite to the theoretical ones.

Acknowledgements. We thank Drs. I. de la Rosa. C. Pérez and M. A. Gigosos for their help. S. González for his work in the experimental device; the Dirección General de Investigación Científica y Técnica (Ministerio de Educación y Ciencia) of Spain for its financial support under Contract No. PB-94-0216. and also the Consejería de Educación y Cultura de la Junta de Castilla y León (VA23-99). Dr. J. A. Aparicio wants to express his personal acknowledgement to the Organización Nacional de Ciegos de Espana (ONCE) for its help.

References

Aparicio J.A., Gigosos M.A., S. Mar, 1997, J. Phys. B 30, 3141
del Val J.A., 1997, In: Medida de Parametros Atomicos en Plasmas de Neon, Ph.D. Thesis, Universidad de Valladolid
del Val J.A., Aparicio J.A., Mar S., 1999, ApJ, 513, 535
del Val J.A., Mar S., Gigosos M.A., et al., 1998, Jpn. J. Appl. Phys. 37, 4177
Gigosos M.A., Cardenoso V., 1996, J. Phys. B 29, 4795
Gigosos M.A., Mar S., Pérez C., de la Rosa I., 1994, Phys. Rev. E 49, 1575
González M.A., González V.R., Mar S., 1989, J. Quant. Spectrosc. Radiat. Transfer 42, 247
Van der Mullen J.A.M., 1990, Phys. Rep. 191, 109